Geotechnical Aspects of Underground Construction in Soft Ground – Viggiani (ed)
© 2012 Taylor & Francis Group, London, ISBN 978-0-415-68367-8

Effects of tunnelling on a single pile: Three-dimensional design tool

J.Q. Surjadinata & T.S. Hull
GHD-Geotechnics, Sydney, Australia

J.P. Carter
University of Newcastle, Newcastle, Australia

ABSTRACT: In most tunnelling projects in urban areas, a preliminary assessment is often required of the impact of a tunnel excavation on foundations adjacent to the tunnel. Despite the significant recent advances in computer hardware and commercial software, a full 3-D analysis is still relatively costly, especially if it is to be employed as a preliminary assessment tool to ascertain the impact of tunnel excavation on existing foundations. This paper provides a convenient and cost-effective design tool, in the form of design charts, that will allow an economical preliminary assessment of the 3-D effects of tunnelling on a single pile. The method adopted to develop these design charts will be briefly described and their use in practice will be illustrated by application of the design charts to several published case histories.

1 INTRODUCTION

Recently there has been an increasing interest in adopting three-dimensional (3-D) numerical analysis to assist in the design and planning of tunnelling projects. This is partly driven by the increasing accessibility of high-powered computing hardware and the convenience offered by modern CAD-based commercial software, which together enable ease of input and output of the often complex 3-D geometry involved in a tunnelling problem.

In tunnelling projects in urban areas, a preliminary assessment is often required of the impact of a tunnel excavation on foundations adjacent to the tunnel. The 3-D geometry of the tunnel and the adjacent foundations commonly found in urban areas may prohibit the use of a conventional plane strain approximation of the problem. In particular, for a tunnel excavation next to existing pile foundations there is increasingly a need for full 3-D analysis.

Despite recent significant advances in computer hardware and commercial software, full 3-D analysis is still relatively costly when employed as a preliminary assessment tool to ascertain the impact of tunnel excavation on existing pile foundations. A cost effective and convenient alternative for preliminary assessment are design chart solutions that can provide a first-order elastic prediction of the pile response due to adjacent tunnel excavation.

Currently, there is only the published design chart of Loganathan et al. (2001) which provides a plane strain solution of pile response to tunnel excavation. However, due to the plane strain nature and the limited pile-tunnel arrangements considered in the Loganathan solution, a 3-D solution that takes into account a larger range of pile and tunnel arrangements would be useful.

Surjadinata (2009) conducted a study of the 3-D response of a pile due to tunnelling. Part of the outcome consisted of 3-D design charts for the response of a single pile due to tunnelling.

This paper provides a brief description of the method adopted by Surjadinata (2009) to develop the 3-D design charts. Their use in practice is then illustrated by application of the design charts to two published case histories.

2 TUNNELLING INDUCED PILE RESPONSE

The design charts were based on an extensive 3-D parametric study of the tunnelling-induced response of a single (wished-in-place) elastic pile, assuming a homogenous isotropic linear elastic soil. To overcome the need to perform full 3-D analysis for every case in the study, the efficient combined Finite-and-Boundary-Element Analysis (FAB) method was employed. The method is based on two stages of analysis. The first stage is to predict the elastic free-field soil displacement induced by a tunnel excavation. This displacement is then used as input to a special boundary element analysis (Hull, 1998) of an elastic pile to obtain the response of the pile. This method has been verified against several existing case studies ranging from existing numerical predictions to back analyses of measured pile response. Further details of the FAB method and the verification of the FAB method can be found in Surjadinata *et al.* (2005, 2006).

It was shown that the maximum elastic pile response due to tunnelling is primarily dependant on the following parameters:

- Ground loss (ε)
- Diameter of the tunnel (D)
- Normalised tunnel depth (H/D)
- Normalised pile length (L_p/H)
- Normalised pile distance (W/D)
- Pile stiffness relative to the soil (L_c/L_p)
- Pile slenderness ratio (L_p/d)
- Position of tunnel face relative to the pile axis (S)

where L_c is the corresponding effective pile length. (Further details of L_c can be found below).

The definition of ground loss (ε) adopted is the reduction in volume of a circular tunnel, expressed as a percentage of the initial excavated tunnel volume.

The geometrical representation of the parameters above, with the exception of L_c, can be found in Figure 1 and a comment on the significance of each parameter is provided below.

From the parametric study it was found that the magnitude of the lateral and vertical responses of the pile attain a maximum value at the plane strain condition ($S\rightarrow\infty$). As the tunnel passes the pile, S = 0, the magnitude of the longitudinal response of the pile attains its maximum value. These maximum responses are presented for the three non-dimensional tunnel depths investigated in this study, i.e., H/D = 2, 3 and 5. These normalised depths will be referred to as "shallow", "intermediate" and "deep", respectively. The magnitudes of the responses are considered for three different pile lengths relative to the tunnel depth (L_p/H = 0.5, 1 and 2). The three pile lengths will be referred to as "short", "intermediate" and "long".

The parameter L_c is the effective or critical length of the pile. L_c is used in this study to define the pile to soil relative stiffness and it is normalised with pile length (L_p). Parameter L_c/L_p is essentially K_R from Poulos and Davis (1980). Detailed explanation of L_c can be found in Poulos (1982) and Hull (1987).

For completeness, the equations for L_c suggested by Hull (1987) are adopted for this study:

$$L_{cB} = \pi\sqrt{2}\left(\frac{(EI)_p}{E_s}\right)^{\frac{1}{4}} \tag{1}$$

$$L_{cA} = \sqrt{\frac{\pi(EA)_p}{E_s}} \tag{2}$$

where L_{cB} = the effective pile length for bending in the lateral and longitudinal directions, L_{cA} = the effective pile length for axial load, $(EI)_p$ = pile bending stiffness, $(EA)_p$ = pile axial stiffness, and E_s = the appropriate soil Young's modulus.

The individual relationships of the parameters listed above (W/D, L_c/L_p, and L_p/d) with the magnitudes of the maximum pile responses in 3 directions, i.e., lateral displacement (U_{xmax}), vertical displacement (U_{ymax}), longitudinal displacement (U_{zmax}), lateral bending moment (M_{xmax}), longitudinal bending moment (M_{zmax}), and axial force (F_{ymax}) were discussed in Surjadinata (2009) and will not be repeated here. Using these relationships, it is possible to generate a system of design charts that provides the maximum magnitude of an elastic pile response due to tunnelling.

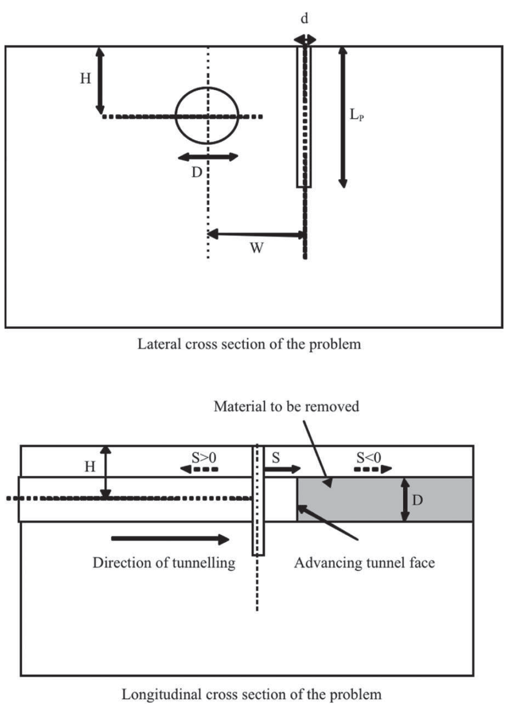

Figure 1. Problem geometry.

3 CREATION OF DESIGN CHARTS

The minimum number of charts required to summarise a particular maximum pile response (e.g., M_{xmax}) is three. These three charts make up a set and are referred to as a "3-chart design set". Each set will correspond to a particular pile response, and a particular pile length (L_p/H = 0.5, 1 or 2).

This means for each pile length, six different 3-chart sets provide the 3-D maximum pile responses. The complete 18 design chart sets are provided in Surjadinata (2009) and interpolation between these charts enables typical pile-tunnel geometries to be evaluated. For illustration purposes, only 2 sets (i.e., U_{xmax} and M_{xmax} for $L_p/H = 2$) will be presented and they can be found in Figures 4 and 7, respectively.

In an elastic analysis, the pile responses due to tunnelling are proportional to the ground loss (ε) and therefore all maximum pile responses will be normalised against ε.

A brief summary of the creation and features of each chart in the 3-chart design set is provided below.

3.1 *Results of 3-D study*

Based on the parametric study, Figure 2 shows the normalised 3-D pile displacement profiles for a pile adjacent to a tunnel. Each displacement profile in a chart corresponds to a different tunnel diameter (D). This figure shows that the pile displacements in three directions can be normalised by D. Note that the normalised vertical displacement in Figure 2(b) is for a different tunnel-pile arrangement than that corresponding to the normalised horizontal displacement, in order to illustrate that the normalisation is valid for any tunnel-pile arrangement. Note that z is the vertical position measured from the tunnel axis, upwards is positive.

Figure 3 shows the normalised pile bending moments and axial force for a pile adjacent to a tunnel. Figures 3(a) and (c) show that the pile bending moment in the lateral and longitudinal directions can be conveniently normalised against $(EI)_p/D$. Figure 3(b) shows that the axial force induced in the pile can be normalised against $(EA)_pL_p/D$.

3.2 *"Reference" chart*

Using the normalisation procedures described above, the first chart in the 3-chart set, referred to as a "reference" chart was created. An example of a reference chart is the first (top) chart in Figures 4 and 7.

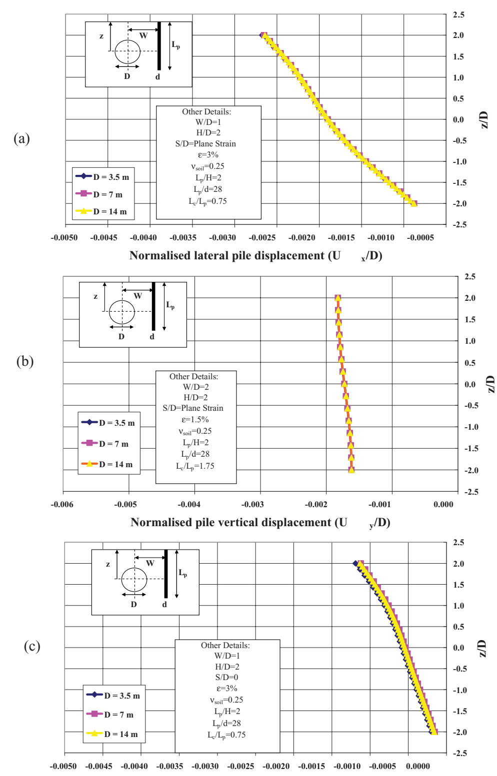

Figure 2. Normalised pile displacement profiles.

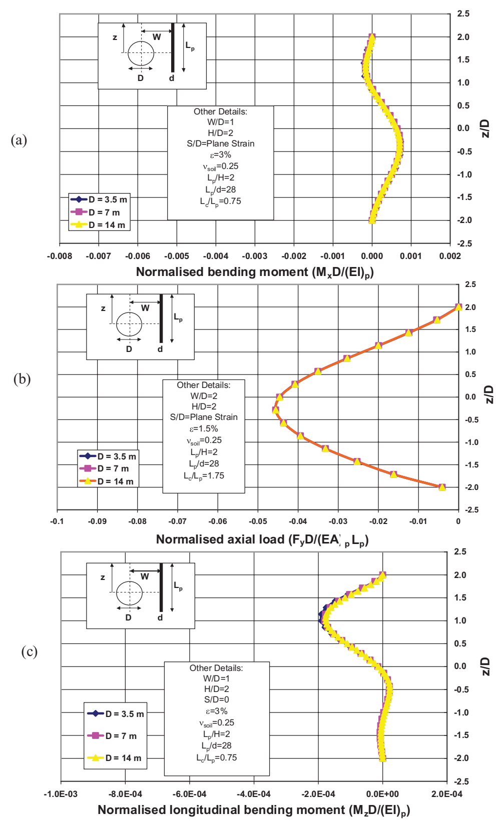

Figure 3. Normalised axial force and bending moment.

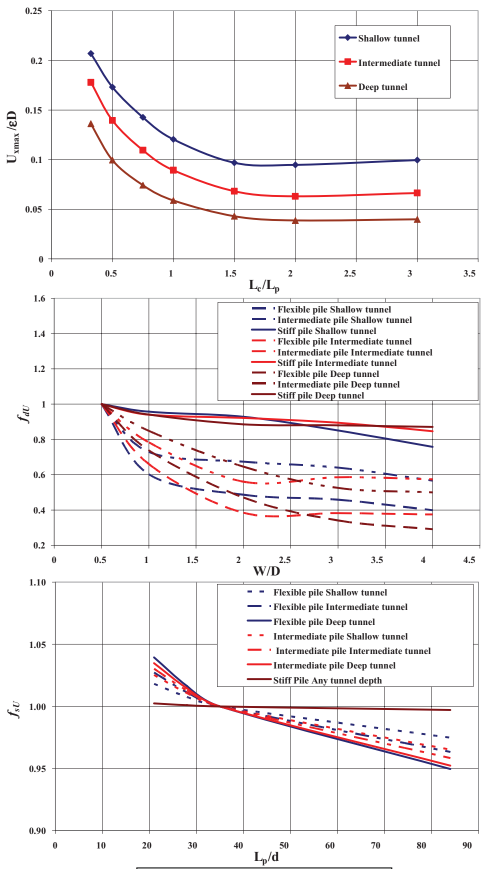

$L_c/L_p \le 0.5$ Flexible pile
$0.5 < L_c/L_p \le 1.0$ Intermediate pile
$L_c/L_p > 1.0$ Stiff pile

Figure 4. Maximum lateral displacement design charts set for $L_p/H = 2$ (Long pile).

In each "reference" chart there are three curves that correspond to a maximum pile response for the three tunnel depths considered (shallow, intermediate and deep). For each pile response, the "reference" chart shows the normalised maximum pile response plotted against L_c/L_p.

In all of the "reference" charts in this study, parameters W/D and L_p/d are kept constant (W/D = 0.5 and $L_p/d = 35$). To take into account other values of W/D and L_p/d, correction factors are applied to the normalised pile responses obtained from the "reference" charts. These correction factors are denoted as f_d and f_s, and they take into account other values of W/D and L_p/d, respectively. The charts that provide the values of f_d and f_s are called auxiliary charts.

The correction factors employ a second letter in the subscript: U indicates displacement, M indicates bending moment and F indicates axial force. Hence, f_{dU} is for displacement, f_{dM} is for bending moment, and f_{dF} is for axial force.

3.3 *First auxiliary chart*

The first auxiliary chart contains the correction factor f_d plotted against the pile distance ratio (W/D), with values of f_d provided for the three pile stiffnesses (flexible, intermediate and stiff) and the three tunnel depths (shallow, intermediate and deep). An example of this chart is the second (middle) chart in Figures 4 and 7.

3.4 *Second auxiliary chart*

The second auxiliary chart contains the correction factor f_s plotted against the pile slenderness ratio (L_p/d). Similar to f_d, values of f_s are provided for the three pile stiffness values and the three tunnel depths. An example of this chart is the third (bottom) chart presented in Figures 4 and 7.

4 LIMIT OF APPLICATION

The application of the proposed design charts is limited to L_c/L_p values presented in the "reference" charts. Specifically, it is not recommended to extrapolate the values of the design charts for cases with L_c/L_p below 0.3 or beyond 3.

5 DESIGN CHARTS GUIDE

In order to use the design charts to obtain the magnitude of the maximum pile response, the steps to be taken are:

1. Establish the values of L_p/H, ground loss (ε in %), the diameter of tunnel (D), L_c/L_p, W/D and L_p/d.
2. Choose the figure (3-chart set) that corresponds to the pile response in question and the value of L_p/H determined in step 1.
3. From the reference chart in the set, read the normalised magnitude of the maximum pile response (at W/D = 0.5 and $L_p/d = 35$).
4. From the auxiliary charts read off the multiplication factors f_d and f_s that take into account the different values of W/D and L_p/d.
5. The magnitude of the maximum pile response can be found by the following equations:

$$U_{x,y\,or\,z\,max} = U^* \times \varepsilon D \times f_{dU} \times f_{sU} \tag{3}$$

$$M_{x\,or\,z\,max} = M^* \times \varepsilon \times \frac{(EI)_p}{D} \times f_{dM} \times f_{sM} \tag{4}$$

$$F_{ymax} = F^* \times \varepsilon \times (EA)_p \times \frac{L_p}{D} \times f_{dF} \times f_{sF} \tag{5}$$

where U* = normalised displacement value (read from the relevant reference chart), M* = normalised bending moment value (read from the relevant reference chart), F* = normalised axial force value (read from the relevant reference chart), $f_{dU}/f_{dM}/f_{dF}$ = correction factors obtained from the first auxiliary chart in the design chart set and $f_{sU}/f_{sM}/f_{sF}$ = correction factors obtained from the second auxiliary chart in the design chart set.

6 APPLICATION OF DESIGN CHARTS

Due to space limitations, only estimates of the full-scale measurements of lateral pile response due to tunnelling will be shown below. Application of the design charts for pile response in the other directions can be found in Surjadinata (2009).

There appear to be only two detailed full-scale measurements of lateral pile response due to tunnelling reported in the literature (Lee et al., 1994 and Pang et al., 2006) prior to 2009. These cases are used to illustrate the level of agreement between the predictions from the design charts, the full-scale measurements in the field and also the numerical predictions presented in the published case studies.

6.1 *Angel underground station in London—background*

The first field case was published by Lee et al. (1994) with data obtained during the construction of a tunnel for the Angel Underground Station in London. The excavation of the tunnel involved two construction steps. Firstly, a pilot tunnel with a diameter of 4.5 m was excavated and this was followed by enlargement of the pilot tunnel to a diameter of 8.25 m. The tunnel centre line is 15 m from the surface. Mair (1993) reported that the ground loss for the pilot tunnel was estimated to be 1.5% and that an additional ground loss of 0.5% occurred due to the pilot tunnel enlargement. The soil profile reported by Lee et al. (1994) shows linearly increasing undrained shear strength from about 50 kPa at the surface to approximately 220 kPa at 30 m depth. An average undrained shear strength (s_u) of 135 kPa was assumed, which is typically associated with a soil Young's modulus of approximately 54 MPa (400 s_u). This value of soil modulus was adopted for the design chart-based prediction and that of Loganathan (1999).

The pile of interest was located 5.7 m away from the tunnel axis with a length of 28 m and a diameter of 1.2 m. Inclinometers were installed within the pile to measure its lateral deflection (U_{xmax}). A cross-sectional view of this case history can be found in Figure 5.

6.2 *Angel underground station in London—analysis*

The step-by-step calculation of U_{xmax}, using the proposed design charts, is as follows:

1. Pilot tunnel contribution
   - L_p/H = 1.86 (adopt L_p/H = 2 chart set)
   - H/D = 3.33 (Intermediate tunnel)
   - εD = 1.5% × 4.5 m = 0.0675 m
   - W/D = 1.267
   - L_c/L_p = 0.452 (Flexible pile)
   - L_p/d = 23.33
   - U^* = 0.18 (Figure 4—Reference chart)
   - f_{dU} = 0.55 (Figure 4—Auxiliary chart 1)
   - f_{sU} = 1.02 (Figure 4—Auxiliary chart 2)

$$U_{xmax} = U^* \times \varepsilon \times D \times f_{dU} \times f_{sU}$$

$$U_{xmax} = 0.18 \times 0.00675 \times 0.55 \times 1.02$$

$$U_{xmax} = 0.0068 \text{ m} = 6.8 \text{ mm}$$

2. Tunnel enlargement contribution
   - L_p/H = 1.86 (adopt L_p/H = 2 chart set)
   - H/D = 1.82 (Shallow tunnel)
   - εD = 0.5% × 8.25 m = 0.04125 m
   - W/D = 0.69
   - L_c/L_p = 0.452 (Flexible pile)
   - L_p/d = 23.33
   - U^* = 0.21 (Figure 4—Reference chart)
   - f_{dU} = 0.78 (Figure 4—Auxiliary chart 1)
   - f_{sU} = 1.02 (Figure 4—Auxiliary chart 2)

$$U_{xmax} = U^* \times \varepsilon \times D \times f_{dU} \times f_{sU}$$

$$U_{xmax} = 0.21 \times 0.04125 \times 0.78 \times 1.02$$

$$U_{xmax} = 0.0069 \text{ m} = 6.9 \text{ mm}$$

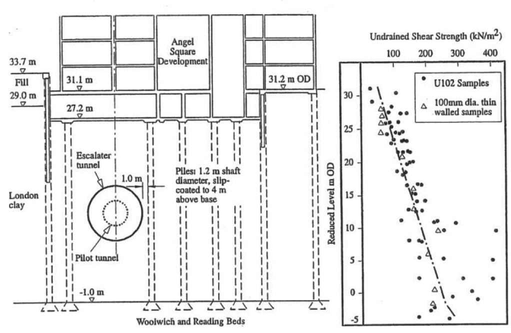

Figure 5. Cross-sectional view of Angel underground station case study (after Lee et al., 1994).

The final U_{xmax} prediction is obtained by superposition of the two separate analyses described above:

$$U_{xmax} = 6.8 + 6.9\ \text{mm} = 13.7\ \text{mm}$$

6.3 *Angel underground station in London—discussion*

Lee et al. (1994) reported that a maximum lateral deflection (U_{xmax}) of the pile of 10 mm was measured at the depth of the tunnel axis. They also provided a plane strain FEM prediction which indicated that U_{xmax} at this depth would have been 20 mm. Loganathan's (1999) design charts predict the position of U_{xmax} to be slightly above the depth of the tunnel axis with a magnitude of 11.9 mm.

The prediction obtained from the proposed design charts is therefore conservative and differs by 13% from the prediction based on the Loganathan (1999) design charts. This is considered reasonable agreement between the proposed design charts and the existing solution.

The difference between the prediction of the design charts and the measured lateral pile displacement (Lee et al., 1994) is relatively small at 3.7 mm, suggesting that as a first-order approximation the proposed design charts are capable of providing reasonable predictions of the pile response in this case.

6.4 *MRT north-east line C704 in Singapore—background*

The second field case was published by Pang et al. (2006) with data obtained during the construction of twin parallel tunnels (North-bound and South-bound) for the MRT (Mass Rapid Transport) North East line C704 in Singapore. Both tunnels were excavated at a depth of 21 m by EPB (Earth Pressure Balance) machines, each 6.5 m in diameter. The pile group was situated between the twin tunnels. Each pile has a diameter of 1.2 m and a Young's modulus of 28 GPa was used to represent the pile stiffness. The geometry of this problem, including sectional and plan views of the pile group, is shown in Figure 6. Further details of this problem can be found in Pang et al. (2006).

The pile group of interest reported by Pang et al. (2005 & 2006) is Pier 20. This pier rests upon a group of four piles, as can be seen in Figure 6. The pile in this group used for comparison purposes was designated P1 by Pang et al. (2005 & 2006) and its position can be seen in Figure 6. It is located very close to the South-bound tunnel with only 1.6 m clear distance between the side of the tunnel and the side of the pile. The clear distance

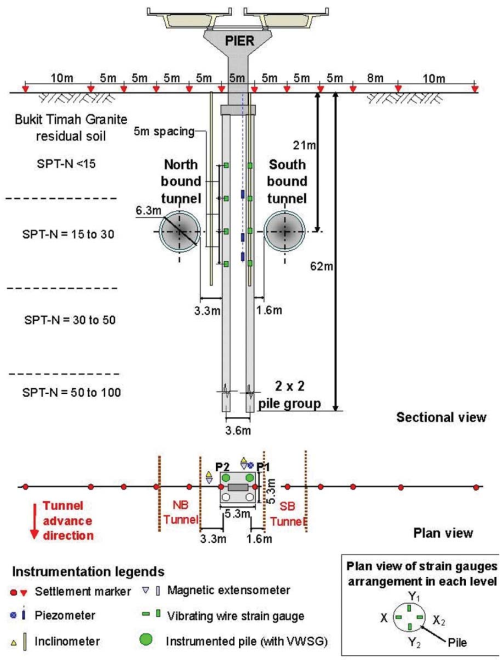

Figure 6. Geometry of MRT N-E line C704 Singapore (after Pang et al., 2006).

between the side of the North-bound tunnel and the side of pile P1 is 6.9 m. The measured ground loss ε from the South-bound tunnel is 1.38%.

Pang et al. (2005) also provided a non-linear 3-D FEM prediction of the maximum response of pile P1. For the FEM analysis, Pang et al. (2005) adopted a multi-layered soil model with a strain dependant Modified Cam Clay formulation developed by Dasari (1996). In this formulation, prior to yielding, the soil stiffness varies with strain.

Pang et al. (2006) note that the pile is mainly embedded in completely weathered (residual soil) Bukit Timah granite. For the predictions using the proposed design charts, it was assumed that the residual soil is uniform with a stiffness of 8.25 MPa (Hefny et al., 2004).

6.5 *MRT north-east line C704 in Singapore—analysis*

Pang et al. (2006 & 2005) provided measurements and FEM predictions of the maximum responses of pile P1. They are the induced lateral and longitudinal bending moments (M_{xmax} & M_{zmax}) and the induced axial force (F_{ymax}). Due to space constraints, only the measurement of maximum lateral bending moment (M_{xmax}) will be compared against the prediction obtained using the proposed design charts.

Note that the measured pile responses are due to ground loss from the South-bound tunnel only.

The step-by-step calculation of the maximum lateral bending moment using the chart solutions is as follows:

South-bound tunnel contribution

L_p/H = 2.9 (adopt L_p/H = 2 chart, see note below)
H/D = 3.23 (Intermediate tunnel)
ε/D = 1.38%/6.5 m = 0.002123 m^{-1}
$(EI)_p$ = 28000 MPa × 0.10178 m^4 = 2850.0 M Nm^2
W/D = 0.838
L_c/L_p = 0.316 (Flexible pile)
L_p/d = 50.8
M^* = 0.29 (Fig. 7)
f_{dM} = 0.46 (Fig. 7)
f_{sM} = 0.95 (Fig. 7)

$$M_{xmax} = M^* \times (EI)_p \times \frac{\varepsilon}{D} \times f_{dM} \times f_{sM}$$

$$M_{xmax} = 0.29 \times 2850 \times 0.002123 \times 0.45 \times 0.95$$

$$M_{xmax} = 0.75 \text{ MNm}$$

Note that the pile length for this case is beyond $L_p/H = 2$ and the design chart for $L_p/H = 2$ was used in the calculation above. This serves as an illustration that for any pile length (L_p/H) beyond 2, the design chart set for $L_p/H = 2$ is the applicable design chart set. The reason is that the maximum portion of pile length that is significantly affected by the tunnel's presence appears to be limited to twice the depth of the tunnel (2H), as observed in Surjadinata (2009).

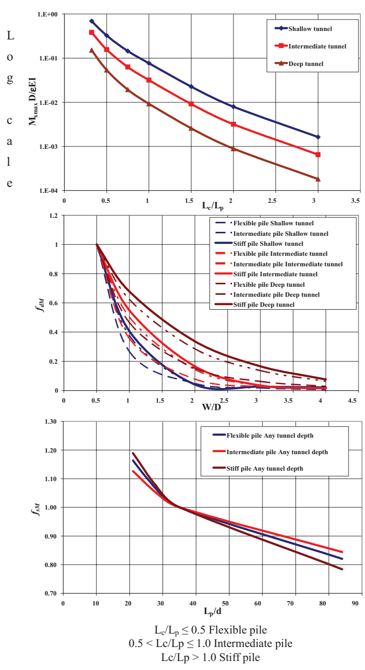

Figure 7. Maximum lateral bending moment design charts set for Lp/H = 2 (Long pile).

6.6 *MRT north-east line C704 in Singapore—discussion*

The measured value of M_{xmax} of pile P1 at the tunnel axis level reported by Pang et al. (2006) was 0.403 MNm and the prediction using the proposed design charts solution is 0.75 MNm. The difference between the measured M_{xmax} and the prediction from the design charts is expected since there are two fundamental differences between the assumed model and reality.

The first difference is due to the fact that the measured value of M_{xmax} is for a pile within a pile group, while the design charts were created for a free-standing single pile. Since the stiffness of a pile connected to the other piles in the group by a (relatively) rigid pile cap might be expected to be higher than a free-standing pile, it is expected that the measured pile response will be lower than the prediction obtained from the proposed design charts. Hence, the values of M_{xmax} predicted for a pile in a group are expected to be less than those of a single free standing pile.

The second difference is that the measured M_{xmax} is for a pile embedded in a layer of soil of increasing stiffness with depth, while the proposed design charts were created for a pile embedded in elastic soil with uniform stiffness. Generally in this case, elastic analysis will provide a conservative prediction of M_{xmax}.

Hence, it is expected that the measured maximum responses of pile P1 will be less than the corresponding predictions from the proposed design charts.

The 3-D non-linear elastoplastic FEM prediction of M_{xmax} reported by Pang et al. (2005) for the same pile (P1) at the level of tunnel axis is 0.6 MNm and, as shown above, the prediction using the proposed design charts solution is 0.75 MNm.

This difference is expected due to the fact that the FEM approach modelled features such as the rigidity of the pile group, layered soil, non-linear elastoplastic soil model and the details of the rate of tunnel advancement, while the design chart solution is for a single pile within a uniform linear elastic soil.

Despite these differences, the proposed design charts provide a reasonable and conservative first order prediction of M_{xmax}, relative to both the measured value and the non-linear FEM prediction.

As further indication of the agreement between the chart prediction and the measured data, though not presented in detail here, employing the charts gave predictions of M_{zmax} = 0.17 MNm and F_{ymax} = 4.05 MN in comparison with the measured values of M_{zmax} = 0.16 MNm and F_{ymax} = 3.4 MN presented in Pang et al. (2006). Complete comparison of Pang et al. data and predictions obtained using the proposed design charts can be found in Surjadinata (2009).

7 ADVANTAGES OF THE DESIGN CHARTS

The main advantage of the proposed design chart system is that it will allow predictions of the pile responses to be made with little cost (in time and effort) relative to existing numerical methods. Given the reasonable degree of agreement with both existing solutions and field measurements of pile response, the proposed design charts should allow cost-effective first-order predictions to be made with some confidence.

Furthermore, if a more refined estimate of the maximum pile behaviour is needed, the first-order estimates from the proposed design charts can be used as a "point of reference" for a more sophisticated numerical analysis.

Another advantage of the proposed design charts relative to other methods published to date is their ability to predict the maximum pile response in the third (longitudinal) direction. To the best knowledge of the authors there are no other published design charts that are able to provide predictions of this type.

Due to all of these advantages, it is therefore considered that the proposed design chart solutions can be comfortably adopted as a preliminary 3-D design tool.

8 SUMMARY

A brief summary of the generation and organisation of design charts for singles piles subjected to the effects of tunnelling was presented. This was followed by a step-by-step guide to using the proposed design charts and a discussion on the limitations of the design charts. Then the application of the proposed design charts to two well-known cases studies was presented in order to illustrate the degree of agreement between the predictions from the design charts, other theoretical methods (FE and other design charts) and measured pile responses. The application of the design charts in these cases indicated that they provide reasonable and conservative predictions.

It is concluded that given the advantages of the design charts solutions, they can reasonably be adopted as a preliminary 3-D design tool.

As additional full scale data become available, more comparisons of the design chart results will be possible and this should allow a better (and more complete) assessment of their predictive capabilities.

REFERENCES

Dasari, G.R. (1996). Modelling the variation of soil stiffness during sequential construction. *PhD thesis*, Cambridge University.

Hefny, A.M. and Lo, K.Y. (1999). Analytical solutions for stresses and displacement around tunnels driven in cross-anisotropic rocks. *Int. J. Numer. Anal. Meth. Geomech*., 23, pp 161–177.

Hull, T.S. (1987). The behaviour of laterally loaded piles. *PhD Thesis*, Department of Civil Engineering, The University of Sydney.

Hull, T.S. (1998). Manual for computer program PALLAS. Centre for Geotechnical Research, The University of Sydney.

Lee, R.G., Turner, A.J. and Whitworth, L.J. (1994). Deformations caused by tunnelling beneath a piled structure. *Proc. XIII Int. Conf. Soil mechanics and Foundation Engineering*, New Delhi, India, pp 873–878.

Loganathan, N. (1999). Effect of tunnelling adjacent to pile foundations. *Ph.D Thesis*, Department of Civil Engineering, The University of Sydney, Australia.

Loganathan, N., Poulos, H.G. and Xu, K.J. (2001). Ground and pile-group responses due to tunnelling. *Soils and Foundations*, 41(1), pp 57–67.

Mair, R.J. (1993). Developments in geotechnical engineering research: application to tunnels and deep excavations Unwin memorial Lecture 1992. *Proc. Instn. Civ. Engrs*, 93, pp 27–41.

Pang, C.H., Yong, K.Y. and Chow, Y.K. (2005). Three-dimensional numerical simulation of tunnel advancement on adjacent pile foundation, *Proceedings of the 31st ITA-AITES World Tunnel Congress*, 7–12 May 2005, Istanbul, Turkey.

Pang, C.H., Yong, K.Y., Chow, Y.K. and Wang, J. (2006). The response of pile foundations subjected to shield tunnelling, *Proceedings of the 5th International Conference of TC28 of the ISSMGE*, Netherlands, pp 737–743.

Poulos, H.G. (1982). "Developments in the analysis of static and cyclic lateral response of piles." *Proc., 4th Int. Conf. on Numerical Methods in Geomechanics*, Canada, 1117–1135.

Poulos, H.G. and Davis, E.H. (1980). Pile Foundation Analysis and Design, New York, John Wiley & Son.

Surjadinata, J.Q., Carter, J.P., Hull, T.S., Poulos, H.G. (2005). Analysis of effects of tunneling on single piles. *Proceedings of 5th International Conference of TC28 of the ISSMGE,* Netherlands, pp 665–671.

Surjadinata, J.Q., Carter, J.P., Hull, T.S., Poulos, H.G. (2006). Combined Finite-and-Boundary-Element analysis of the effects of tunneling on single piles. *International Journal of Geomechanics*, Vol 6 No. 5, pp 374–377.

Surjadinata, J.Q. (2009). The Influence of tunneling on single piles. *Ph.D Thesis*, Department of Civil Engineering, The University of Sydney, Australia.